A MIMO Detector With Deep Learning in the Presence of Correlated Interference

Junjuan Xia, Ke He, Wei Xu, Shengli Zhang, Lisheng Fan, and George K. Karagiannidis, *Fellow, IEEE*

***Abstract*—In this paper, we investigate the classical detection problem for vehicle networks with multiple antennas, by considering practical communication scenarios, where the interfering signals are correlated over time or frequency. In such cases, the conventional detector requires to estimate the joint distribution of the interfering signals, which imposes a huge computational complexity. To tackle this issue, we propose the joint use of a maximum likelihood detector (MLD) and a deep convolutional neural network (DCNN), where MLD is used to produce an initial detection result and DCNN improves the detection by exploiting the local correlation to suppress the interference. Furthermore, the improved DCNN is enhanced by devising the loss function through the cross-entropy of the detection, which can help to suppress the interfering signals and simultaneously force the residual interference to approach the Gaussian distribution. Simulation results are presented to verify the effectiveness of the proposed detector compared to the conventional one. The trained model and source code for this work are available at https://github.com/skypitcher/project_dcnnmld.**

***Index Terms*—Vehicle networks, correlated interfering signals, DCNN.**

I. Introduction

In vehicle networks, the multiple-input multiple-output (MIMO) technique can effectively support the demands for high data-rate, due to the advantage of spatial diversity. To detect the transmitted signals at the MIMO receiver, several techniques have been proposed, such as the maximum likelihood detector (MLD), minimum mean square error (MMSE) and zero-forcing (ZF) [1]. Most of the existing detection algorithms are model-driven, and require the knowledge of the distribution of interference. However, in some communication scenarios, the distribution of interference is very complicated, and not analytically tractable, or it is hard to find a model to fit the distribution [2]. In these cases, the conventional model-driven detectors fail to perform well, which motivates us to investigate new detectors for the MIMO systems in the presence of complicated interference.

Recently, there has been a high interesting on the use of artificial intelligence (AI) in wireless communications, due to the explosively increasing capability of computation [3]–[7]. In contrast to the traditional model-driven, the data-driven algorithms in AI can adaptively learn how to design the wireless systems through collected data. Regarding the literature in this research area, the authors in [8] proposed a novel and effective deep learning approach for non-orthogonal multiple access (NOMA) systems, which significantly improve the system performance and reduce the computational burden. In [9], the authors applied convolutional neural networks (CNNs) for automatic modulation classification, which could achieve much higher accuracy. The works in [8], [9] provide critical guidance for the application of AI in wireless communications. Furthermore, the authors in [10] used reinforcement learning algorithms in wireless networks to improve the security. In the case of correlated interference environments, the authors in [11] proposed a novel iterative belief propagation-CNN network framework for channel decoding, which reduces significantly the decoding error probability. For the signal detection in MIMO systems, two deep learning based neural networks have been proposed by researchers, i.e., the detection network (DetNet) and MMNet [12]–[14], which can approach the detection performance of MLD, especially for the massive MIMO systems.

As another kind of deep learning algorithm, unfolded message passing (MP) algorithm and the associated networks have recently attracted much attention from researchers in the filed of wireless communications [15]–[19]. Specifically, the MP algorithm was applied for MIMO-NOMA systems in [15], and it was found that iterative LMMSE detection could achieve the Gaussian capacity of MIMO system for Gaussian signaling. Moreover, it was proved that approximate message passing (AMP) receiver could achieve the constrained capacity of MIMO systems for the phase and amplitude modulation schemes [16], [17]. In [18] and [19], the authors analyzed the convergence and performance of the loopy message passing receiver. In [17], the authors proposed a deep learning based orthogonal AMP detector, OAMP-Net, by unfolding the iterative OAMP algorithm, which improves the performance of the iterative algorithm significantly under Rayleigh and correlated MIMO channels. Overall, MLD and these deep learning based detectors, such as the DetNet, MMNet and OAMP-Net, perform the symbol-by-symbol detection, and cannot exploit the correlation among different symbols over time or frequency domain, which motivates the work in this paper.

In this paper, we investigate the MIMO detection problem in the presence of correlated interference over time or frequency. An important component of the interference is interfering signals, which may arise due to aggressive reuse of frequency resources in the wireless networks. In practice, when the symbol duration of the interfering users is several times that of the desired users, then the interfering signals are correlated in the time domain [2]; for an orthogonal frequency division multiplexing (OFDM) system, the temporal residual interference leads to correlated interference in the frequency domain, especially when the synchronization and channel estimation are not perfect [1]. Overall, the interference may be correlated in practice, which makes the conventional model-driven detectors fail to perform well. To deal with the detection problem of MIMO systems in the presence of correlated interference, we propose a framework of MLD and DCNN, where the DCNN exploits the correlation features to suppress the interference. Moreover, the performance of DCNN can be improved by devising the loss function through the cross-entropy of the detection, which not only suppress the interfering signals but also forces the residual interference to approach the Gaussian distribution. Simulation results in the presence of correlated interference are demonstrated to verify the effectiveness of the proposed detector.

Manuscript received July 13, 2019; revised October 21, 2019, December 18, 2019, and February 3, 2020; accepted February 4, 2020. Date of publication February 10, 2020; date of current version April 16, 2020. This work was supported in part by the NSFC under Grants 61871139, 61871109, and 61941115, in part by the Science and Technology Program of Guangzhou under Grant 201807010103, and in part by the Graduate Innovative Research Grant Program of Guangzhou University under Grant 2019GDJC-M18. The review of this article was coordinated by Dr. B. Mao. *(Corresponding authors: Ke He; Lisheng Fan.)*

Junjuan Xia, Ke He, and Lisheng Fan are with the School of Computer Science, Guangzhou University, Guangzhou 510000, China (e-mail: xiajunjuan@gzhu.edu.cn; 2111806022@e.gzhu.edu.cn; lsfan@gzhu.edu.cn).

Wei Xu is with the National Mobile Communications Research Laboratory, Southeast University, Nanjing 210096, China (e-mail: wxu@seu.edu.cn).

Shengli Zhang is with the College of Information Engineering, Shenzhen University, Shenzhen 518060, China (e-mail: zsl@szu.edu.cn).

George K. Karagiannidis is with the Aristotle University of Thessaloniki, 54 124 Thessaloniki, Greece (e-mail: geokarag@auth.gr).

Digital Object Identifier 10.1109/TVT.2020.2972806

II. System Model

Generally, we assume a MIMO communication system in a vehicle network in the presence of correlated interference, with M_T antennas at the transmitter and M_R antennas at the receiver. Quadrature Phase shift keying (QPSK) modulation is adopted at the transmitter. The $M_T \times 1$ transmitted signal vector $\mathbf{s}$ is transmitted through the $M_R \times M_T$ MIMO time-varying fading channel. There are N symbols in a transmission packet, and at the n-th symbol ($1 \leq n \leq N$), the received signal can be described by:

$$\mathbf{y}(n) = \mathbf{H}(n)\mathbf{s}(n) + \mathbf{w}(n), \tag{1}$$

where the $M_R \times 1$ vector $\mathbf{w}(n) \in \mathcal{C}N(\mathbf{0}, \sigma^2\mathbf{I})$ is the additive interfering signal and $\mathbf{H}(n)$ denotes the channel matrix at the n-th symbol, in which each element is subject to $\mathcal{C}N(\mathbf{0}, 1)$. If the interfering signals are independent among different symbols, the standard MLD can be employed to detect the transmitted signals symbol-by-symbol as,

$$\hat{\mathbf{s}}(n) = \arg\min_{\mathbf{s}_i \in \Omega} \|\mathbf{y}(n) - \mathbf{H}(n)\mathbf{s}_i\|^2, \tag{2}$$

where Ω is the set of all possible transmitted signals. Note that the detection complexity in (2) increases exponentially with M_T. If the additive interferences $\mathbf{w}(n)$ are correlated with each other, then the optimal detector is a maximum likelihood sequential detector (MLSD) [1],

$$\{\hat{\mathbf{s}}(1), \ldots, \hat{\mathbf{s}}(N)\} = \arg\max_{\{\mathbf{s}(1),\ldots,\mathbf{s}(N)\} \in \Omega^N} \Pr(\mathbf{s}(1), \ldots, \mathbf{s}(N) | \mathbf{y}(1), \ldots, \mathbf{y}(N)), \tag{3}$$

where Ω^N denotes the candidate set of the N transmitted signals. The sequential detector in (3) has a huge computational complexity which increases exponentially with $M_T N$. Moreover, the MLSD requires the joint distribution of $\{\mathbf{w}(n) | 1 \leq n \leq N\}$, which is very difficult to be estimated. Even for the correlation coefficients among symbols, it is still hard to be estimated in practice, especially when the correlation is time-variant. Hence, it becomes almost impossible to implement the MLSD due to the lack of a tractable expression for interference, e.g, $\mathbf{w}$, thus losing its optimality in applications even putting aside the exponentially increasing complexity.

III. An Improved DCNN Based MIMO Detector

In this section, we present the the iterative architecture of DCNN-MLD for MIMO detection. After discussing the design of both the baseline and improved implementation of the network, we analyze the computation complexity of the whole architecture.

A. An Iterative DCNN-MLD Framework

In order to overcome the limitations of the sequential detector in (3), we propose an improved framework of DCNN-based MLD (DCNN-MLD), which is depicted in Fig. 1.

In Fig. 1(a), the standard symbol-by-symbol MLD and the improved DCNN are jointly used, where there are K iterations between MLD and the DCNN. At each round of iteration, the MLD firstly outputs the estimation of the transmitted signal $\hat{\mathbf{s}}(n)$ as described in (2). From $\hat{\mathbf{s}}(n)$, we can obtain an initial estimate of the interference, denoted by $\hat{\mathbf{w}}(n)$, as

$$\hat{\mathbf{w}}(n) = \mathbf{y}(n) - \mathbf{H}(n)\hat{\mathbf{s}}(n). \tag{4}$$

Based on $\hat{\mathbf{w}}(n)$, DCNN then outputs a more accurate estimate of the interference, denoted by $\tilde{\mathbf{w}}(n)$, by capturing the features inherent in the interfering signals, especially about the local correlation among

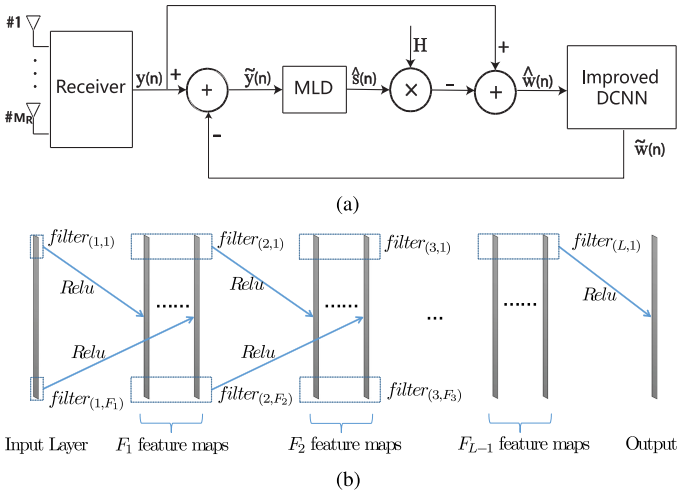

Fig. 1. Improved detection framework of DCNN based MLD. (a) Improved DCNN based MLD. (b) Structure of improved DCNN.

different symbols. After that, the output of the DCNN $\tilde{\mathbf{w}}(n)$ is fed back to MLD, and we can obtain the input signal of the MLD for the next round of iteration, denoted by $\tilde{\mathbf{y}}(n)$, as,

$$\tilde{\mathbf{y}}(n) = \mathbf{y}(n) - \tilde{\mathbf{w}}(n) \tag{5}$$

$$= \mathbf{H}(n)\mathbf{s}(n) + \mathbf{w}(n) - \tilde{\mathbf{w}}(n) \tag{6}$$

$$\triangleq \mathbf{H}(n)\mathbf{s}(n) + \mathbf{z}(n), \tag{7}$$

where $\mathbf{z}(n) = \mathbf{w}(n) - \tilde{\mathbf{w}}(n)$ represents the effective residual interference.

Fig. 1(b) shows the structure of the improved DCNN consisting of L convolutional layers only, where the first convolutional layer is an input layer, followed by $L-2$ hidden layers, and the last one is the output layer. The input layer is convolved with F_1 filters with filter size of R_1, denoted by $\{filter_{(1,f_1)} | f_1 \in [1, F_1]\}$. Accordingly, the input layer generates F_1 feature maps through the convolutional operation. Then, these F_1 feature maps are input to the second convolutional layer, which consists of F_2 filters with filter size of R_2, denoted by $\{filter_{(2,f_2)} | f_2 \in [1, F_2]\}$. Overall, the l-th layer ($1 \leq l \leq L$) contains F_l filters with filter size of R_l, and this layer will obtain the F_{l-1} feature maps produced by the prior layer and then output F_l feature maps for the next layer. This process repeats until the final output layer is used. The last convolutional layer is convolved with only one filter, since the output feature should have the same dimension with the input data. By summarizing the parameters in the improved DCNN, we can denote the structure of the DCNN as $\{L; R_1, R_2, ..., R_L; F_1, F_2, ..., F_L\}$.

B. A Baseline Implementation of DCNN

In DCNN, the loss function plays a critical role in controlling the learning direction and updating the network parameters. In this paper, the goal of loss function is to train the DCNN to output an estimation of interference $\tilde{\mathbf{w}}(n)$ that benefits the MLD in (2). A direct way is to make the output of DCNN $\tilde{\mathbf{w}}(n)$ approach to the expected interference $\mathbf{w}(n)$ as much as possible. Accordingly, a typical MSE-based loss function is given by,

$$f_a = \frac{\sum_{n=1}^{N} \sum_{j=1}^{M_R} ||z_j(n)||^2}{M_R N}, \tag{8}$$

which can minimize the power of the residual interference $\mathbf{z}(n)$ and serve as a baseline for the performance of the proposed DCNN.

Note that the baseline DCNN in (8) focuses on suppressing the interfering signals only, and it ignores the distribution of the residual interference in the training process. When the distribution of effective interference $\mathbf{z}(n)$ deviates from the Gaussian distribution, the detector in (2) can fail. For non-Gaussian interference, the detection performance deteriorates. This severely limits the detection performance of the baseline DCNN-MLD. In order words, if we intend to improve the detection result further, we should suppress the interference $\mathbf{z}(n)$ and meanwhile force its distribution to approach Gaussian distribution as much as possible.

C. An Improved Implementation of DCNN

To overcome the limitation of DCNN-MLD, we employ the results of detection to devise an improved loss function for the DCNN. Since the detection result depends on both the power and the distribution of the residual interfering signals $\mathbf{z}(n)$, the training process should jointly exploit both the information of $\mathbf{z}(n)$ to tune the DCNN parameters. To implement the improved DCNN, we first need to calculate the likelihood of the correct candidate among all possible ones. To facilitate this, we apply the SoftMax function [20] to smooth the detection function in (2) in order to make it derivative with respect to $\mathbf{s}_i$. We use $q_i(n)$ to denote the probability that a candidate $\mathbf{s}_i$ ($\mathbf{s}_i \in \Omega$) is correct for the n-th observation, given by [20],

$$q_i(n) = \frac{e^{-\|\mathbf{y}(n)-\tilde{\mathbf{w}}(n)-\mathbf{H}(n)\mathbf{s}_i\|^2}}{\sum_{j=1}^{|\Omega|} e^{-\left\|\mathbf{y}(n)-\tilde{\mathbf{w}}(n)-\mathbf{H}(n)\mathbf{s}_j\right\|^2}}, \tag{9}$$

where $|\Omega|$ denotes the cardinality of Ω. Since the signal detection problem is a classification one, we use the one-hot (aka one-of-K) scheme [21] to represent the categorical data. Then, the corresponding probabilities of all candidates for the n-th observation can be denoted by,

$$\mathbf{Q}(n) = [q_1(n), q_2(n), \ldots, q_{|\Omega|}(n)], \tag{10}$$

where $\mathbf{Q}(n)$ satisfies the condition of $\sum_{i=1}^{|\Omega|} q_i(n) = 1$. Moreover, for the n-th observation, we use $p_i(n)$ to represent the value that the corresponding $q_i(n)$ is expected to be. The value of $p_i(n)$ can be obtained by labeling in the training set through one-hot encoding, and $p_i(n)$ is equal to 1 if the candidate $\mathbf{s}_i$ is correct or zero otherwise. From $p_i(n)$, the expected values of $\mathbf{Q}(n)$ is denoted by,

$$\mathbf{P}(n) = [p_1(n), p_2(n), \ldots, p_{|\Omega|}(n)], \tag{11}$$

which satisfies the condition of $\sum_{i=1}^{|\Omega|} p_i(n) = 1$.

From the information theory, the cross-entropy is commonly used to quantify the difference between two probability distributions over the same underlying event sets [22]. Accordingly, for distributions of $q_i(n)$ and $p_i(n)$, we write the cross-entropy between $\mathbf{Q}(n)$ and $\mathbf{P}(n)$ as [1]

$$C(n) = \sum_{i=1}^{|\Omega|} p_i(n) \log_2 \frac{1}{q_i(n)}, \tag{12}$$

which measures the detection error at the n-th symbol. The cross-entropy $C(n)$ decreases when the detection is improved. In particular, $C(n)$ achieves its minimum value when the distribution $\mathbf{P}(n)$ is exactly the same as the estimated distribution $\mathbf{Q}(n)$. By applying (9) into (12), we constitute an improved loss function for the DCNN as:

$$f_e = \frac{1}{N}\sum_{n=1}^{N} C(n) \tag{13}$$

$$= \frac{1}{N}\sum_{n=1}^{N}\sum_{i=1}^{|\Omega|} p_i(n) \log_2 \frac{\sum_{j=1}^{|\Omega|} e^{-\left\|\mathbf{y}(n)-\tilde{\mathbf{w}}(n)-\mathbf{H}(n)\mathbf{s}_j\right\|^2}}{e^{-\|\mathbf{y}(n)-\tilde{\mathbf{w}}(n)-\mathbf{H}(n)\mathbf{s}_i\|^2}}. \tag{14}$$

Compared with the baseline loss function, the improved loss function in (13) employs the detection result in the training process, which relies on both the power and distribution of the residual interference $\mathbf{z}(n)$. In other words, the power and distribution of $\mathbf{z}(n)$ can both tune the parameters in the DCNN. Hence, the improved DCNN can help to suppress the interfering signals and simultaneously force the residual interference to approach the Gaussian distribution, which therefore improved the detection performance of the DCNN-MLD.

From the above description, we can summarize several major differences between the baseline and improved DCNN. The first difference is the loss function, which acts as a kernel function in the deep neural networks. Due to the difference in the loss function, the baseline DCNN focuses on suppressing the interference power, while the improved DCNN also incorporates the interference distribution, which constitutes the second difference. As a result, the result of well-trained parameters between the baseline and improved DCNN is different, which leads to a significant difference in the detection performance between the baseline and improved DCNN.

D. Computational Complexity Analysis

In this subsection, we describe the required computational complexity caused by the iterative DCNN-MLD framework with K iterations. The conventional MLD algorithm with QPSK modulation needs the computational complexity of $O(4^{M_T})$ for each iteration. In addition, since the DCCN is composed of multiple convolutional layers, its computational complexity comes from the operation of convolution and the number of layers. For the DCCN setting in this paper, the computational complexity at each iteration is equal to $O(\sum_{l=1}^{L}(F_{l-1}R_l N F_l))$ [23]. In summary, the total computational complexity of the iterative DCNN-MLD framework with K iterations equals to $O((K+1)4^{M_T} + K\sum_{l=1}^{L}(F_{l-1}R_l N F_l))$. From this expression, we can find that the computational complexity of the iterative DCNN-MLD detection framework increases almost linearly with the number of iterations.

IV. Simulation Results and Discussions

In this section, we present some simulation results to verify the effectiveness of the improved DCNN-MLD detector. The parameter setting in this work is summarized in Table I. Specifically, there are four antennas at the transmitter and receiver, with $M_T = M_R = 4$. QPSK modulation is adopted in this work and each transmission packet consists of 576 bits [11], so that $N = 72$. In addition, the channel matrix is time-varying and we apply a typical model, namely the Jakes model [24], to generate the channel matrix with the normalized Doppler frequency f_d setting to 0.1. [2] Moreover, we employ a typical temporal

[1] For two distributions p and q, the cross-entropy $H(p,q)$ is a term of KL divergence $D_{KL}(p,q)$, given by $D_{KL} = H(p,q) - H(p)$. For a given distribution p, $H(p,q)$ and $D_{KL}(p,q)$ differ only by a constant factor for all q. Therefore, we use the cross-entropy instead of KL divergence to avoid some unnecessary computations.

[2] Note that the proposed method in this work can be applied to other kinds of channels, such as Nakagami-m and Rician channels. In this case, the generated training data has been changed, and accordingly, we should re-train the model to detect the signals.

TABLE I
PARAMETER SETTING

Parameter	Value
M_T	4
M_R	4
Modulation scheme	QPSK
N	72
f_d	0.1
K	3
L	4
$\{R_1, R_2, R_3, R_4\}$	$\{36, 3, 3, 36\}$
$\{F_1, F_2, F_3, F_4\}$	$\{32, 16, 8, 1\}$
Mini-batch size	720
Number of training batches	20,000
Number of valid batches	10,000
Number of test batches	10,000

correlation model to generate the correlated interfering signals [1],

$$\mathbf{w}(n+1) = \sqrt{\rho}\mathbf{w}(n) + \sqrt{1-\rho}\mathbf{u}(n+1), \tag{15}$$

where $\mathbf{u}(n+1) \in \mathcal{CN}(\mathbf{0}, \sigma^2)$ is an additive noisy term independent of $\mathbf{w}(n)$, and $\rho \in [0, 1]$ denotes the correlation coefficient of the interfering signals. In particular, $\rho = 0$ and $\rho = 1$ correspond to the uncorrelated and completely correlated scenarios, respectively. Regarding the DCNN structure, we use four convolutional layers with $L = 4$, where the number of convolutional filters at the four layers are set to 32, 16, 8 and 1, respectively. Moreover, the filter size at the four layers is set to 36, 3, 3 and 36, respectively.

As to the data set for simulation, we set the training set to contain 20,000 batches, which are used to train the learnable variables inside the filters through the mini-batch gradient descent technique [25]. Moreover, the valid set and test set both contain 10,000 batches, which are used to validate the generalization ability during the training process and test the performance after completing the training, respectively. Each batch contains 10 packets, and each packet consists of 72 data units, so that the mini-batch size is equal to 720. Each data unit contains the received signal and the channel parameters. In the training process, the transmitted signal is also included in the data unit as the label, in the form of one-hot encoded vector.

Fig. 2 shows the effect of correlation coefficient of the interfering signals on the detection performances of MLD, the baseline and improved DCNN-MLDs, where the transmit signal-to-interference ratio (SIR) is set to 10 dB. The correlation coefficient ρ varies from 0 to 0.9, where $\rho = 0$ and $\rho = 0.9$ correspond to the uncorrelated and highly correlated scenarios, respectively. We can find from Fig. 2 that the detection BER performances of the baseline and improved MLD improve with a larger value of ρ. This is because that the DCNN based MLD can help suppress the interfering signals through exploiting the local correlation among interferences, and the DCNN can capture the local correlation characteristic better when the correlation among interfering signals increases. Moreover, the improved DCNN-MLD outperforms the MLD and baseline DCNN-MLD, especially when the interfering signals are highly correlated. In particular, when $\rho = 0.8$ where the interfering signals are highly correlated, the improved DCNN-MLD with $K = 2$ can reduce the detection error of the standard MLD to about 2%, and reduce that of the baseline DCNN-MLD with $K = 2$ to about 30%. In further, we can find that both the performances of baseline DCNN-MLD and improved DCNN-MLD become better with K enlarges, which indicates that the iterative DCNN-MLD framework can take advantage of the iteration between MLD and DCNN. As the computational complexity of the iterative DCCN-MLD detection

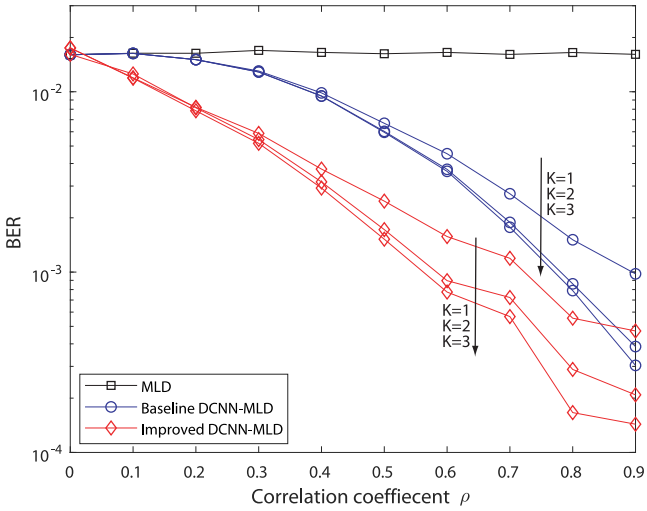

Fig. 2. Effect of the correlation coefficient of the interfering signals on the detection performance.

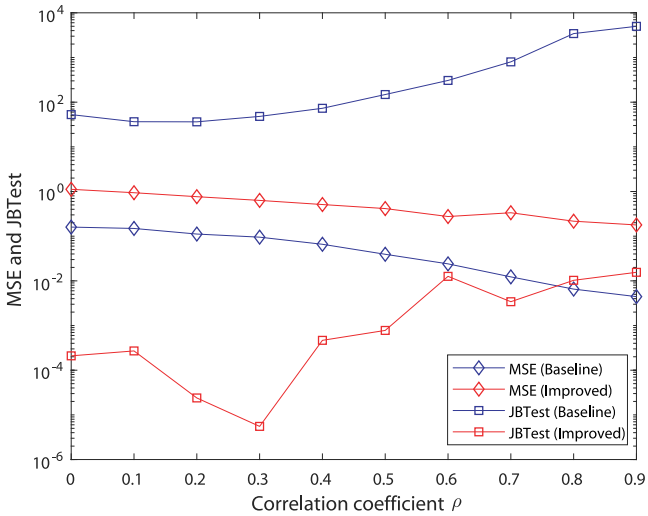

Fig. 3. MSE and JBTest of the baseline and improved DCNN-MLDs with $K = 2$.

increases almost linearly with the number of iteration, we select to set K to 2, in the subsequent figures, by taking into account both the detection performance and computational complexity.

To reveal the inherent mechanism for the results in Fig. 2 and explain why the improved DCNN-MLD has better performance, Fig. 3 is provided under the same parameter settings with Fig. 2. In this figure, we use the mean squared error (MSE) of the effective interference $\mathbf{z}(n)$ to indicate how similar the output of DCNN $\tilde{\mathbf{w}}$ is to the underlying interference $\mathbf{w}$, and employ Jarque-Bera test (JBTest) [26] to characterize how well the effective interference $\mathbf{z}(n)$ matches with the Gaussian distribution. We can see from Fig. 3 that compared with the improved DCNN, the baseline DCNN has lower MSE, while it has much higher JBTest value. That indicates that the baseline DCNN concentrates on suppressing the interfering signals only, while it ignores the distribution of interferences. In contrast, the improved DCNN can suppress the interfering signals and simultaneously force the residual interference to approach the Gaussian distribution, which reveals the inherent mechanism for the BER performance comparison in Fig. 2.

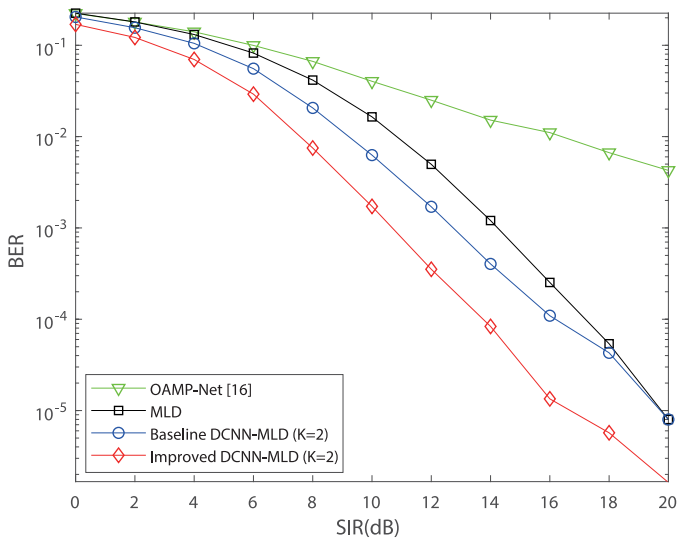

Fig. 4. BER performances comparison versus SIR with $\rho = 0.5$.

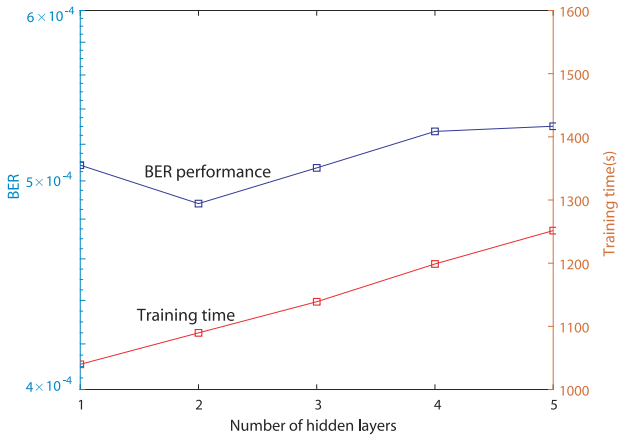

Fig. 5. BER performance and training time of the improved DCNN-MLD versus the number of hidden layers.

Fig. 4 demonstrates the BER performances of MLD, the baseline and improved CNN-MLDs, where $\rho = 0.5$, $K = 2$ and the transmit SIR varies from 0 dB to 20 dB. For comparison, we also plot the BER performance of OAMP-Net based detector [17] in this figure. As observed from Fig. 4, we can find that the improved DCNN-MLD outperforms the OAMP-Net, MLD and baseline DCNN-MLD in a wide range of SIR, and the performance improvement enlarges with the increasing value of SIR. In particular, the SIR gains of the improved DCNN-MLD over the standard MLD and the baseline DCNN-MLD are 4 dB and 2 dB, respectively, at the BER level of 10^{-3}. This further validates the effectiveness of the improved DCNN-MLD.

Fig. 5 shows the BER performance and required training time of the improved DCNN-MLD versus the number of hidden layers, where $\rho = 0.8$, SIR=10 dB, $K = 2$, and the number of hidden layers in the DCNN varies from 1 to 5. The filter size at each layer is the same as the size in Figs. 2–4. Note that increasing the number of hidden layers can be regarded as an efficient way to increase the total number of parameters in the DCNN. As observed from Fig. 5, we can find that when the network is deeper with an increasing number of hidden layers, the training time becomes larger indicating that it becomes more difficult to train the parameters in the network. Moreover, the BER performance is improved when the number of hidden layers increases from 1 to 2, since more layers can help capture the interference correlation characteristics among different symbols. However, too many parameters will cause the training result inaccurate due to inefficient back propagation of gradients in deep networks [8], [9], which leads to a poorer BER. By taking into account both the BER performance and training time, we can validate that it is reasonable to set the number of hidden layers to 2 in Figs. 2–4.

V. Conclusion

In this paper, we have proposed an improved DCNN-based MLD in the vehicle networks, for the classical MIMO signal detection problem in the presence of correlated interference,where the MLD and improved DCNN were jointly used. MLD was used to estimate the transmitted signals and DCNN to improve the detection result by suppressing the interfering signals by exploiting the local correlation. The improved DCNN was devised by using the loss function, which is based on the cross-entropy of the detection result. This can help to suppress the interfering signals and simultaneously force the residual interference to approach the Gaussian distribution. Simulation results over different scenarios of correlated interfering signals were demonstrated to show the superiority of the improved DCNN-MLD over the standard MLD and the baseline DCNN-MLD. In future works, we will study other kinds of deep neural networks [27]–[29] to exploit the local correlation among interfering signals, in order to further enhance the detection performance for the considered system.

References

[1] J. G. Proakis, *Digital Communications*, 5th ed. New York, NY, USA: McGraw-Hill, 2008.
[2] M. Haenggi and R. K. Ganti, "Interference in large wireless networks," *Found. Trends Netw.*, vol. 3, no. 2, pp. 127–248, 2009.
[3] B. Mao *et al.*, "A novel non-supervised deep-learning-based network traffic control method for software defined wireless networks," *IEEE Wireless Commun.*, vol. 25, no. 4, pp. 74–81, Aug. 2018.
[4] Z. M. Fadlullah, B. Mao, F. Tang, and N. Kato, "Value iteration architecture based deep learning for intelligent routing exploiting heterogeneous computing platforms," *IEEE Trans. Comput.*, vol. 68, no. 6, pp. 939–950, Jun. 2019.
[5] J. Xia and D. Deng, "A note on implementation methodologies of deep learning-based signal detection for conventional MIMO transmitters," *IEEE Trans. Broadcast.*, to be published.
[6] B. Mao *et al.*, "Routing or computing? The paradigm shift towards intelligent computer network packet transmission based on deep learning," *IEEE Trans. Comput.*, vol. 66, no. 11, pp. 1946–1960, Nov. 2017.
[7] Y. Wang, J. Yang, M. Liu, and G. Gui, "LightAMC: Lightweight automatic modulation classification using deep learning and compressive sensing," *IEEE Trans. Veh. Technol.*, vol. 69, no. 3, pp. 3491–3495, Mar. 2020.
[8] G. Gui, H. Huang, Y. Song, and H. Sari, "Deep learning for an effective nonorthogonal multiple access scheme," *IEEE Trans. Veh. Technol.*, vol. 67, no. 9, pp. 8440–8450, Sep. 2018.
[9] Y. Wang, M. Liu, J. Yang, and G. Gui, "Data-driven deep learning for automatic modulation recognition in cognitive radios," *IEEE Trans. Veh. Technol.*, vol. 68, no. 4, pp. 4074–4077, Apr. 2019.
[10] L. Xiao, D. Jiang, D. Xu, H. Zhu, Y. Zhang, and H. V. Poor, "Two-dimensional anti-jamming mobile communication based on reinforcement learning," *IEEE Trans. Veh. Technol.*, vol. 67, no. 10, pp. 9499–9512, Oct. 2018.
[11] F. Liang, C. Shen, and F. Wu, "An iterative BP-CNN architecture for channel decoding," *IEEE J. Sel. Topics Signal Process.*, vol. 12, no. 1, pp. 144–159, Feb. 2018.
[12] Z. Li, C. Peng, G. Yu, X. Zhang, Y. Deng, and J. Sun, "Detnet: A backbone network for object detection," pp. 1–12, 2018.
[13] N. Samuel, T. Diskin, and A. Wiesel, "Deep MIMO detection," in *Proc. 18th IEEE Int. Workshop Signal Process. Advances Wireless Commun.*, Jul. 2017, pp. 1–5.

[14] M. Khani, M. Alizadeh, J. Hoydis, and P. Fleming, "Adaptive neural signal detection for massive MIMO," pp. 1–20, 2019.
[15] L. Liu, Y. Chi, C. Yuen, Y. L. Guan, and Y. Li, "Capacity-achieving MIMO-NOMA: Iterative LMMSE detection," *IEEE Trans. Signal Process.*, vol. 67, no. 7, pp. 1758–1773, Apr. 2019.
[16] L. Liu, C. Liang, J. Ma, and L. Ping, "Capacity optimality of AMP in coded systems," pp. 1–8, 2019.
[17] H. He, C.-K. Wen, S. Jin, and G. Y. Li, "A model-driven deep learning network for MIMO detection," in *Proc. IEEE Global Conf. Signal Inf. Process.*, 2018, pp. 584–588.
[18] L. Liu, C. Yuen, Y. L. Guan, Y. Li, and C. Huang, "Gaussian message passing for overloaded massive MIMO-NOMA," *IEEE Trans. Wireless Commun.*, vol. 18, no. 1, pp. 210–226, Jan. 2019.
[19] L. Liu, C. Yuen, Y. L. Guan, Y. Li, and Y. Su, "Convergence analysis and assurance for Gaussian message passing iterative detector in massive MU-MIMO systems," *IEEE Trans. Wireless Commun.*, vol. 15, no. 9, pp. 6487–6501, Sep. 2016.
[20] C. M. Bishop, *Pattern Recognition and Machine Learning (Information Science and Statistics)*, 2006.
[21] D. Harris and S. Harris, *Digital Design and Computer Architecture*. San Mateo, CA, USA: Morgan Kaufmann, 2010.
[22] L. Y. Deng, "The cross-entropy method: A unified approach to combinatorial optimization, Monte-Carlo simulation and machine learning," *Technometrics*, vol. 48, no. 1, pp. 147–148, 2004.
[23] K. He and J. Sun, "Convolutional neural networks at constrained time cost," in *Proc. IEEE Conf. Comput. Vision Pattern Recognit.*, 2015, pp. 5353–5360.
[24] M. K. Simon and M. S. Alouini, *Digital Communication over Fading Channels*, 2nd ed. Hoboken, NJ, USA: Wiley, 2005.
[25] L. Mu, Z. Tong, and S. J. Alexander, "Efficient mini-batch training for stochastic optimization," in *Proc. 20th ACM SIGKDD Int. Conf. Knowledge Discovery Data Mining (KDD)*, New York, NY, USA, Aug. 2014, pp. 661–670.
[26] C. M. Jarque, "Jarque-bera test," in *Proc. Int. Encyclopedia Statist. Sci.*, 2011, pp. 701–702.
[27] J. Xia, "Intelligent secure communication for Internet of Things with statistical channel state information of attacker," *IEEE Access*, vol. 7, no. 1, pp. 144 481–144 488, 2019.
[28] G. Liu, "Deep learning based channel prediction for edge computing networks towards intelligent connected vehicles," *IEEE Access*, vol. 7, pp. 114 487–114 495, 2019.
[29] Z. Zhao, "A novel framework of three-hierarchical offloading optimization for MEC in industrial IoT networks," *IEEE Trans. Ind. Informat.*, to be published, doi: 10.1109/TII.2019.2949348.